Computational study of heat transfer in a conjugate turbulent wall jet flow with constant heat flux

E. Vishnuvardhanarao
Department of Mechanical Engineering, Indian Institute of Technology, Guwahati, India, and
Manab Kumar Das
Department of Mechanical Engineering, Indian Institute of Technology, Kharagpur, India

Received 1 April 2007
Revised 29 October 2007
Accepted 29 October 2007

Abstract

Purpose – The purpose of this paper is to consider the conjugate heat transfer from a flat plate involving a turbulent plane wall jet. The bottom wall of the solid block is heated by a constant heat flux.

Design/methodology/approach – High Reynolds number two-equation model (κ-ϵ) has been used for turbulence modeling. The parameters considered are the conductivity ratio of solid and fluid, the solid slab thickness and the Prandtl number. The Reynolds number considered is 15,000 because the flow becomes fully turbulent and then is independent of the Reynolds number. The range of parameters considered are: conductivity ratio = 1-1,000, solid slab thickness = 1-10 and Prandtl number = 0.01-100.

Findings – The non-dimensional bottom surface temperature is high for high-Prandtl number fluid and vice versa. As conductivity ratio increases, it decreases whereas it increases with the increase in slab thickness. Similar trend is observed for the distribution of the interface temperature. The Nusselt number computed based on the interface temperature increases with Prandtl number. It is observed that for the range of parameters considered, local Nusselt number distribution superimposes with each other. The average heat flux at the interface has been computed and found to be equal with average heat flux at the bottom which ensures the overall heat balance.

Originality/value – The study of conjugate heat transfer with a turbulent wall jet will be useful for cooling of heated body.

Keywords Heat transfer, Turbulence, Simulation, Flow

Paper type Research paper

Nomenclature

$C_{1\epsilon}$, $C_{2\epsilon}$, C_μ	= turbulence model constants	p_0	= ambient pressure
h	= width of the jet	P	= non-dimensional static pressure
k	= turbulent kinetic energy		
K	= thermal conductivity ratio of solid to fluid (k_s/k_f)	Pr	= Prandtl number
		Re	= Reynolds number, $U_0 h/\nu$
$\bar{p}$	= static pressure	S	= thickness of solid slab

International Journal of Numerical Methods for Heat & Fluid Flow
Vol. 19 No. 1, 2009
pp. 39-52

0961-5539
DOI 10.1108/09615530910922143

$\bar{T}$	= dimensional temperature	*Greek symbols*	
T_∞	= inlet and ambient temperature	α_l, α_t	= laminar and turbulent thermal diffusivities, respectively
U_0	= average inlet jet velocity		
$\bar{u}, \bar{v}$	= dimensional mean velocities in x, y-directions, respectively	ϵ	= dissipation
		$\bar{\theta}$	= non-dimensionalized temperature
$\bar{U}, \bar{V}$	= non-dimensional velocities in X, Y-directions, respectively	ν_l, ν_t	= laminar and turbulent kinematic viscosity
x, y	= dimensional co-ordinates		
X, Y	= non-dimensional co-ordinates	σ_k, σ_ϵ	= turbulence model constants

1. Introduction

In a conjugate heat transfer problem, the heat transfer in a fluid regime is coupled with the conducting solid wall having a finite thickness. Equality of the temperature and the heat fluxes at the solid-fluid interface are considered for this case and is referred to as the fourth-kind boundary condition (Luikov *et al.*, 1971). Conjugate heat transfer applies to the thermal systems in which the multi-mode convection/conduction heat transfer is of particular importance to thermal design. Conjugate heat transfer is involved in many applications like high speed jet engines, electronics cooling, film cooling of turbine blades, extrusion of materials, etc.

In the present case, a conjugate heat transfer from a solid block heated with a constant wall flux is con-sidered. It is being cooled by a turbulent plane wall jet. Glauert (1956) has given a similarity solution for plane wall jet as well as radial wall jet for both laminar and turbulent cases are presented with the introduction of Glauert constant F. Seban and Back (1961) have measured and compared the turbulent wall jet velocity profile and the adiabatic wall temperature. The results agree generally with each other. In the laminar flow regime, many publications are devoted to conjugate heat transfer on flat plate details of which may be found in Kanna and Das (2005). However, the conjugate heat transfer study involving a turbulent flow has received little attention. Some of the conjugate heat transfer work published in literature (involving turbulent flow) are by Iaccarino *et al.* (2002), Yilbas *et al.* (2002, 2003), Kassab *et al.* (2003) and Hsieh and Lien (2005).

In the present case, the conjugate heat transfer involving a turbulent plane wall jet is considered. The bottom of the solid slab is heated by a constant heat flux. In the conjugate heat transfer approach, the conduction in the solid and the convection equations in the fluid regions are solved simultaneously. The parameters considered are the conductivity ratio (solid/fluid), the solid slab thickness and the Prandtl number. The Reynolds number considered is 15,000 because the flow becomes fully turbulent and then it becomes independent of the Reynolds number (Holland and Liburdy, 1990).

The near-wall treatments of turbulence models are the key factors to yield an accurate wall heat transfer predictions. In the standard high-Reynolds number κ-ϵ models, wall functions are commonly employed to bridge the turbulent and near-wall viscous regions. Different modifications of the two-equation turbulence models have been used by several researchers to solve the jet impingement problems. For example, Bouainouche *et al.* (1997) have studied the wall shear stress produced by the impingement of a plane turbulent jet on a plate. Heck *et al.* (2001) have solved the gas quenching problem. Merci *et al.* (2003) have solved the heat transfer in the case of jet impingement on to a surface. In the present study, the high-Reynolds number two equation turbulence model with standard wall function has been used to solve the wall jet flow and conjugate heat transfer problem.

2. Governing equations

The schematic diagram of the two-dimensional wall jet with a solid slab is shown in Figure 1. The governing equations are considered to be steady, 2D and incompressible. Thermo-physical properties are assumed to be constant. In the fluid region, the flow is fully turbulent and the Reynolds averaged Navier-Stokes equations are used for predicting the turbulent flow. Boussinesq approximation is used to link the Reynolds stresses to the velocity gradients. The standard κ-ϵ model is used for calculating the turbulent viscosity (v_t). In the solid region, the 2D heat transfer equation is solved. The resulting governing equations in the fluid are:

- continuity equation:

$$\frac{\partial \bar{u}}{\partial x} + \frac{\partial \bar{v}}{\partial y} = 0, \tag{1}$$

- x-momentum equation:

$$\frac{\partial(\bar{u}^2)}{\partial x} + \frac{\partial(\bar{u}\bar{v})}{\partial y} = \frac{1}{\rho}\frac{\partial \bar{p}}{\partial x} + \frac{\partial}{\partial x}\left[(v + v_t)\frac{\partial \bar{u}}{\partial x} - \frac{2}{3}k\right] + \frac{\partial}{\partial y}\left[(v + v_t)\frac{\partial \bar{u}}{\partial y}\right], \tag{2}$$

- y-momentum equation:

$$\frac{\partial(\bar{u}\bar{v})}{\partial x} + \frac{\partial \bar{v}^2}{\partial y} = \frac{1}{\rho}\frac{\partial \bar{p}}{\partial y} + \frac{\partial}{\partial x}\left[(v + v_t)\frac{\partial \bar{v}}{\partial x}\right] + \frac{\partial}{\partial y}\left[(v + v_t)\frac{\partial \bar{v}}{\partial y} - \frac{2}{3}k\right], \tag{3}$$

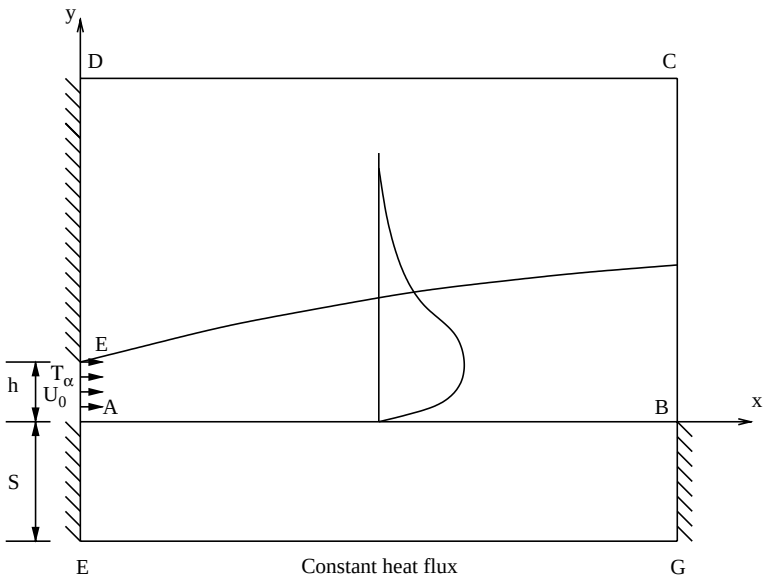

Figure 1.
Schematic and computational domain of the wall jet flow

- energy equation:

$$\frac{\partial(\bar{u}\bar{T})}{\partial x}+\frac{\partial(\bar{v}\bar{T})}{\partial y}=\frac{\partial}{\partial x}\left[(\alpha+\alpha_{\mathrm{t}})\frac{\partial\bar{T}}{\partial x}\right]+\frac{\partial}{\partial y}\left[(\alpha+\alpha_{\mathrm{t}})\frac{\partial\bar{T}}{\partial y}\right]. \tag{4}$$

- Turbulent kinetic energy (k) equation:

$$\frac{\partial(\bar{u}k)}{\partial x}+\frac{\partial(\bar{v}k)}{\partial y}=\frac{\partial}{\partial x}\left[\left(v+\frac{v_t}{\sigma_k}\right)\frac{\partial k}{\partial x}\right]+\frac{\partial}{\partial y}\left[\left(v+\frac{v_t}{\sigma_k}\right)\frac{\partial k}{\partial x}\right]+G-\epsilon. \tag{5}$$

- Rate of dissipation (ϵ) equation:

$$\frac{\partial(\bar{u}\epsilon)}{\partial x}+\frac{\partial(\bar{v}\epsilon)}{\partial y}=\frac{\partial}{\partial x}\left[\left(v+\frac{v_t}{\sigma_k}\right)\frac{\partial\epsilon}{\partial x}\right]+\frac{\partial}{\partial y}\left[\left(v+\frac{v_t}{\sigma_k}\right)\frac{\partial\bar{\epsilon}}{\partial y}\right]+C_{1\epsilon}\frac{\epsilon}{k}G-c_{2\epsilon}\frac{\epsilon^2}{k}. \tag{6}$$

Where production by shear (G):

$$G=v_t\left[2\left(\frac{\partial\bar{u}}{\partial x}\right)^2+2\left(\frac{\partial\bar{v}}{\partial y}\right)^2+\left(\frac{\partial\bar{u}}{\partial y}+\frac{\partial\bar{v}}{\partial x}\right)^2\right]. \tag{7}$$

Eddy viscosity (v_{t}) is given as:

$$v_{\mathrm{t}}=C_\mu\frac{k^2}{\epsilon}. \tag{8}$$

In the solid region, the energy equation is:

$$\left(\frac{\partial^2T}{\partial x^2}+\frac{\partial^2T}{\partial y^2}=0\right). \tag{9}$$

The dimensionless variable are defined as:

$$\begin{aligned}&\bar{U}=\frac{\bar{u}}{U_0},\bar{V}=\frac{\bar{v}}{U_0},X=\frac{\bar{x}}{h},Y=\frac{\bar{y}}{h},\bar{\theta}=\frac{\bar{T}-T_\infty}{T_h-T_\infty}\\&\bar{P}=\frac{\bar{p}-\bar{p}_0}{\rho U_0^2},k_n=\frac{k}{U_0^2},\epsilon_n=\frac{\epsilon}{U_0^3/h},\nu_{\mathrm{t},n}=\frac{\nu_{\mathrm{t}}}{\nu},\alpha_{\mathrm{t},n}=\frac{\alpha_{\mathrm{t}}}{\alpha}.\end{aligned} \tag{10}$$

The non-dimensionalized equations are:

- Continuity equation:

$$\frac{\partial\bar{U}}{\partial X}+\frac{\partial\bar{V}}{\partial Y}=0. \tag{11}$$

- *x*-momentum equation:

$$\frac{\partial \bar{U}^2}{\partial X}+\frac{\partial(\bar{U}\bar{V})}{\partial Y}=\frac{\partial}{\partial X}\left(\bar{P}+\frac{2}{3}k\right)+\frac{1}{Re}\frac{\partial}{\partial X}\left[(1+v_{t,n})\frac{\partial \bar{U}}{\partial X}\right]+\frac{1}{Re}\frac{\partial}{\partial Y}\left[(1+v_{t,n})\frac{\partial \bar{U}}{\partial Y}\right]. \tag{12}$$

- *y*-momentum equation:

$$\frac{\partial(\bar{U}\bar{V})}{\partial X}+\frac{\partial(\bar{V})^2}{\partial Y}=\frac{\partial}{\partial Y}\left(\bar{P}+\frac{2}{3}k\right)+\frac{1}{Re}\frac{\partial}{\partial X}\left[(1+v_{t,n})\frac{\partial \bar{V}}{\partial X}\right]+\frac{1}{Re}\frac{\partial}{\partial Y}\left[(1+v_{t,n})\frac{\partial \bar{V}}{\partial Y}\right]. \tag{13}$$

- Temperature equation ($\bar{\theta}$) is:

$$\frac{\partial(\bar{U}\bar{\theta})}{\partial X}+\frac{\partial(\bar{V}\bar{\theta})}{\partial X}=\frac{1}{RePr}\frac{\partial}{\partial X}\left[(1+\alpha_{t,n})\frac{\partial \bar{\theta}}{\partial X}\right]+\frac{1}{RePr}\frac{\partial}{\partial Y}\left[(1+\alpha_{t,n})\frac{\partial \bar{\theta}}{\partial Y}\right]. \tag{14}$$

- Turbulent kinetic energy (k_n) equation is:

$$\frac{\partial(\bar{U}k_n)}{\partial X}+\frac{\partial(\bar{V}k_n)}{\partial X}=\frac{1}{Re}\frac{\partial}{\partial X}\left[\left(1+\frac{v_{t,n}}{\sigma_k}\right)\frac{\partial k_n}{\partial X}\right]+\frac{1}{Re}\frac{\partial}{\partial Y}\left[\left(1+\frac{v_{t,n}}{\sigma_k}\right)\frac{\partial k_n}{\partial Y}\right]+G_n-\epsilon_n. \tag{15}$$

- Rate of dissipation (ϵ_n)equation is:

$$\frac{\partial(\bar{U}\epsilon_n)}{\partial X}+\frac{\partial(\bar{V}\epsilon_n)}{\partial X}=\frac{1}{Re}\frac{\partial}{\partial X}\left[\left(1+\frac{v_{t,n}}{\sigma_k}\right)\frac{\partial \epsilon_n}{\partial X}\right]+\frac{1}{Re}\frac{\partial}{\partial Y}\left[\left(1+\frac{v_{t,n}}{\sigma_k}\right)\frac{\partial \epsilon_n}{\partial Y}\right]+C_{1\epsilon}\frac{\epsilon_n}{k_n}G_n-C_{2\epsilon}\frac{c^{2/n}}{k_n}. \tag{16}$$

- Production (G):

$$G_n=\frac{v_{t,n}}{\partial X}\left[2\left(\frac{\partial \bar{U}}{\partial X}\right)^2+2\left(\frac{\partial \bar{V}}{\partial Y}\right)^2\left(\frac{\partial \bar{U}}{\partial X}+\frac{\partial \bar{V}}{\partial Y}\right)^2\right]. \tag{17}$$

- Eddy viscosity (v_t, n):

$$v_{t,n} = C\mu Re \frac{k(2/n)}{\epsilon_n}. \tag{18}$$

- Eddy diffusivity (α_t, n):

$$\alpha_{t,n} = \frac{v_{t,n}}{Pr}, \tag{19}$$

where: $\sigma_k = 1.0$, $\sigma_\epsilon = 1.30$, $C_{1\epsilon} = 1.44$, $C_{2\epsilon} = 1.92$, $C_\mu = 0.09$.

In the solid region, the energy equation is:

$$\frac{\partial^2 \theta}{\partial X^2} + \frac{\partial^2 \theta}{\partial Y^2} = 0. \tag{20}$$

3. Numerical scheme and method of solution

In the present work, for the fluid region, the dimensionless governing equations are discretized using the control volume method (Patankar, 1980). Power-law scheme is used to discretize the convective terms and central difference is used for diffusive terms due to ensure the stability of the solution. To avoid the fine mesh required to resolve the viscous sub-layer near the boundary, the wall function method (Launder and Spalding, 1974) has been used which is appropriate for high-Reynolds number flows. SIMPLE (Patankar, 1980) algorithm is followed to solve the finite difference equations. Pseudo-transient approach (Versteeg and Malalasekera, 1996) is used to under-relax the momentum and the turbulent equations. An under-relaxation of 0.2 is used for pressure. In the solid region, central differencing is used for discretizing the energy equation by finite difference technique.

4. Boundary conditions

The jet is entering into the quiescent ambient fluid at the surface of the wall. The non-dimensionalized boundary conditions are provided as input to the solution. At the inlet (AE) of the jet, $U = 1.0$, $V = 0$, $\theta = 0$ are the boundary conditions for the velocities and temperature, respectively. For the turbulent kinetic energy equation, the boundary condition at inlet is $k_n = 1.5I^2$ where I is the turbulence intensity and is equal to 0.02 (Biswas, 2002). For the dissipation equation, the boundary condition at inlet is $\epsilon_n = k_n c((3/4)/\mu)/l$, where $l = 0.07\,\mathrm{h}$ (Biswas, 2002). At the solid wall (DE), no-slip boundary condition is used for velocities and adiabatic condition is used for the temperature. At the entrainment and exit boundaries (i.e. CD and BC, respectively), Neumann boundary conditions are provided, i.e. $\partial\phi/\partial n = 0$ where $\phi = \bar{U}, \bar{V}, \bar{\theta}\, k_n$ and ϵ_n. At the solid-fluid interface (AB), no-slip boundary conditions are applied for velocities and for the temperature, equality of temperature and flux, i.e. $(\theta_s)_w = (\theta_f)_w$ and $(Q_w)_s = (Q_w)_f$ are applied and the details are mentioned in the appendix (Appendix A). Wall functions are used to prescribe the shear stress, production and dissipation rates at the walls. It has been ensured that the first grid falls within the logarithmic region, i.e. $20 \leq Y^+ \leq 60$, where $Y^+ = yu_r/v$, ur being the friction velocity. At the bottom of solid block (i.e. at EG) constant heat flux is applied. The details of constant heat flux is given in Appendix B. Since the both the walls of solid block (i.e. AE and BG), the heat supplied at the bottom of the wall and at the interface must be equal and it is observed.

The code is already tested for validation and grid independence for $Re = 15{,}000$ without solid block. Since the flow is incompressible the already available fluid solution is used to solve the energy equation in both solid and fluid. Grid independence is done in the solid for $S = 1$ by varying the Prandtl number and thermal conductivity ratio (K). For other sizes grid size is correspondingly increased, which is reasonably valid in the solid block.

5. Results and discussion

In the present work, $Re = 15{,}000$ is chosen for all computations. The flow becomes fully turbulent and there is no discernible Reynolds number effect on the mean flow characteristics (Holland and Liburdy, 1990). Since the uniform velocity and some turbulent intensity is given at the inlet of the jet, it takes some length for the flow to become fully turbulent and develop the self similar region, which is observed in the fluid solution. It is observed that approximately at X(30, the flow become fully turbulent and a self-similarity is achieved. At the bottom, a constant heat flux boundary condition is applied. The purpose of the study is to observe and describe the effect of Prandtl number (Pr), thermal conductivity ratio (K) and the thickness of solid slab (S) on the bottom wall temperature, interface surface temperature (θ_i), heat transfer between the solid and the fluid (Q_i), local Nusselt number distribution (Nu_x), average Nusselt number ($\overline{Nu}$) and the temperature distribution in the solid and the fluid. For this, Pr is varied between 0.01 and 100, K is varied between 1 and 1,000 and S is varied between 1 and 10. The derivation of heat flux is given in Appendix A. The definition of constant heat flux at the solid wall is given in Appendix B. The definitions of Nu_x and $\overline{Nu}$ are shown in Appendix C.

5.1 Bottom wall temperature

As discussed in Appendix B, the constant heat flux boundary condition is applied by $-(\partial\theta/\partial Y) = (Pr/K)$ (equation (A5)). Here, Q_b is taken as $1/Re$. For a fixed K, as Pr is increasing, the bottom wall temperature is also increasing (Figure 2(a)). Unlike a constant wall temperature case, the bottom wall temperature is changing with the change in Pr and K. Similarly, as K is increasing, the bottom wall temperature is decreasing (Figure 2(b)). As S increases, the resistance to heat transfer increases. So the bottom wall temperature increases (Figure 2(c)). In the downstream direction Nu_x decreases and thus the bottom wall temperature increases.

5.2 Interface temperature

Figure 3(a) shows the interface temperature (θ_i) distribution at various Prandtl numbers keeping the solid thickness ($S = 10$) and the thermal conductivity ratio ($K = 1{,}000$) constant. Since the bottom wall temperature is high for high Pr case, the interface temperature is also high. The Nu_x is high near the inlet and thus there is decrease of the interface temperature for $Pr = 100$. Similarly, as Pr decreases, the interface temperature also decreases. Figure 3(b) shows the θ_i distribution at various thermal conductivity ratios keeping the Prandtl number equal to 1.0 and solid thickness equal to 10. The interface temperature for the first half is low for low K and the situation reverses for the last half. Figure 3(c) shows the θ_i distribution at various

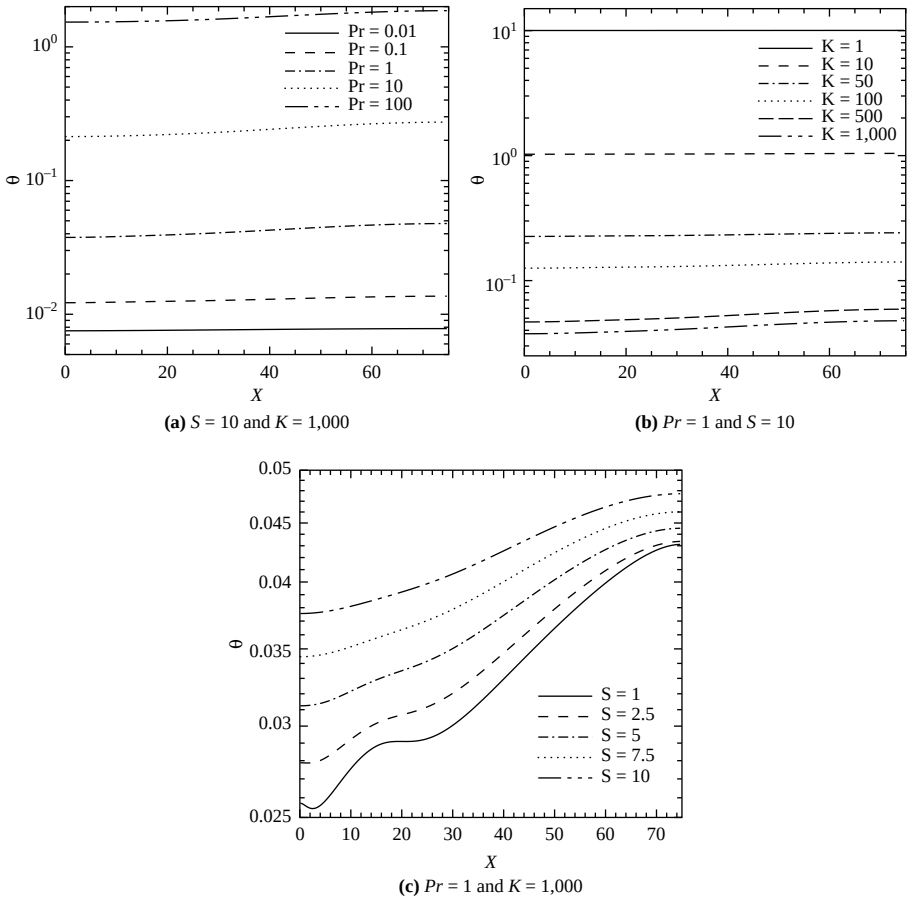

(a) $S = 10$ and $K = 1{,}000$

(b) $Pr = 1$ and $S = 10$

(c) $Pr = 1$ and $K = 1{,}000$

Figure 2.
Bottom surface temperature distribution

solid thicknesses (S) keeping the Prandtl number ($Pr = 1.0$) and thermal conductivity ratio ($K = 1{,}000$). Similar trend is observed in this case also.

5.3 Local Nusselt number

Figure 4(a) shows the Nu_x distribution at various Prandtl numbers keeping the solid thickness ($S = 10$) and thermal conductivity ratio ($K = 1{,}000$) constant. In general, Nu_x increases to a large value near the jet entry and then gradually decreases in the direction of flow. This is a characteristics of the jet boundary layer formation. As shown in the figure, it demonstrates clearly that Nu_x increases with Pr because of the thinning of the thermal boundary layer. Figure 4(b) shows the Nu_x distribution at various thermal con-ductivity ratios keeping $Pr = 1.0$ and $S = 10$. It is observed that for the range of K, the Nu_x distribution superimposes with each other. Figure 4(c) shows the Nu_x distribution at various solid thickness (S) keeping $Pr = 1.0$ and thermal conductivity ratio $K = 1{,}000$. Similar to the previous case, the Nu_x distributions for the range of S superimposes with each other. From these three

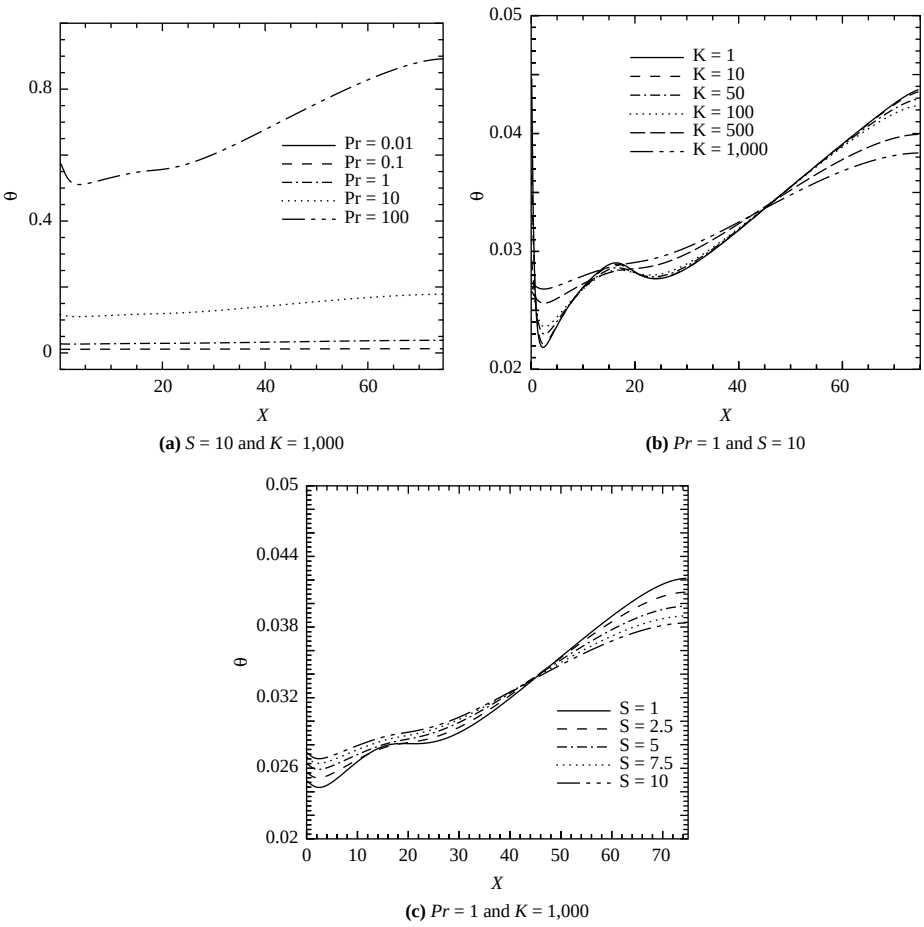

(a) $S = 10$ and $K = 1{,}000$

(b) $Pr = 1$ and $S = 10$

(c) $Pr = 1$ and $K = 1{,}000$

Figure 3.
Interface temperature distribution

figures, it is concluded that Nu_x dependents on the fluid property Pr and remains unaltered for the variation of K and S.

5.4 Local heat flux

Figure 5(a) shows the local heat flux Q_x distribution occurring through the interface at various Prandtl numbers keeping $S = 10$ and $K = 1{,}000$. There are minor variation of heat flux as Pr is being changed. Though a constant heat flux is applied at the bottom of the wall, it is observed that the heat flux along the wall varies at the interface. The local heat flux is high at the inlet and decreases along the wall. The variation of local heat flux is high for low-Prandtl numbers. Figure 5(b) shows the Q_w distribution at various thermal conductivity ratios keeping $Pr = 1.0$ and $S = 10$. At low thermal conductivity ratios the local heat flux along the wall is constant and increases as K increases. The heat flux applied at the bottom is constant. The same heat flux has to pass through the interface. As the heat flux is high in the initial part, the same thus deceases in the later part to satisfy the continuity of heat flux. Figure 5(c) shows the Q_w

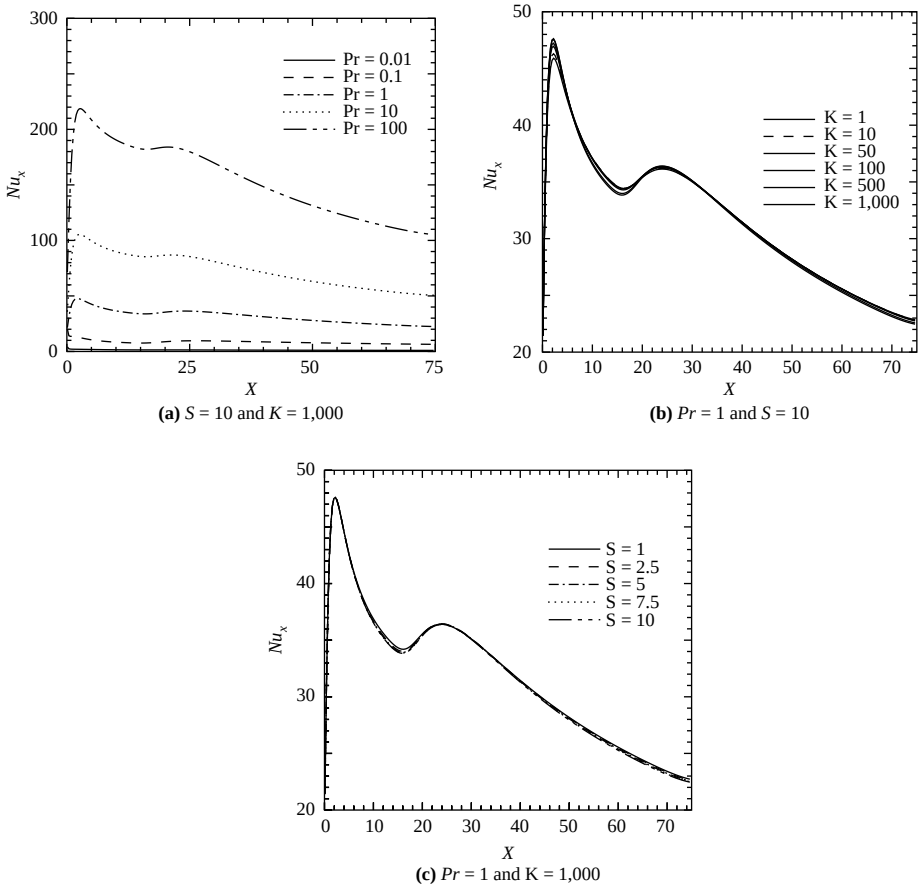

(a) $S = 10$ and $K = 1{,}000$

(b) $Pr = 1$ and $S = 10$

(c) $Pr = 1$ and K = 1,000

Figure 4.
Local Nusselt number distribution

distributions at various solid thickness (S) keeping $Pr = 1.0$ and $K = 1{,}000$. It is found that there is an effect of slab thickness on the local heat flux along the wall. At inlet of the jet, the local heat flux increases as the slab thickness increases. The decrement of heat flux along the later part can be justified by the reason given above.

5.5 Average Nusselt number

Extensive computations are done in the respective ranges of the parameters. The results of the average Nusselt number ($\overline{Nu}$) are presented in Table I. It shows clearly that $\overline{Nu}$ is a function of Prandtl number only. The effect of the solid thickness (S) and the thermal conductivity ratio (K) are negligibly small. It is observed that $\overline{Nu}$ increases with the increase of Pr.

5.6 Average heat transfer

The average heat transfer integrated over the surface for various S, K and Pr are obtained. It has been ensured that the average heat transfer from the interface matches with that

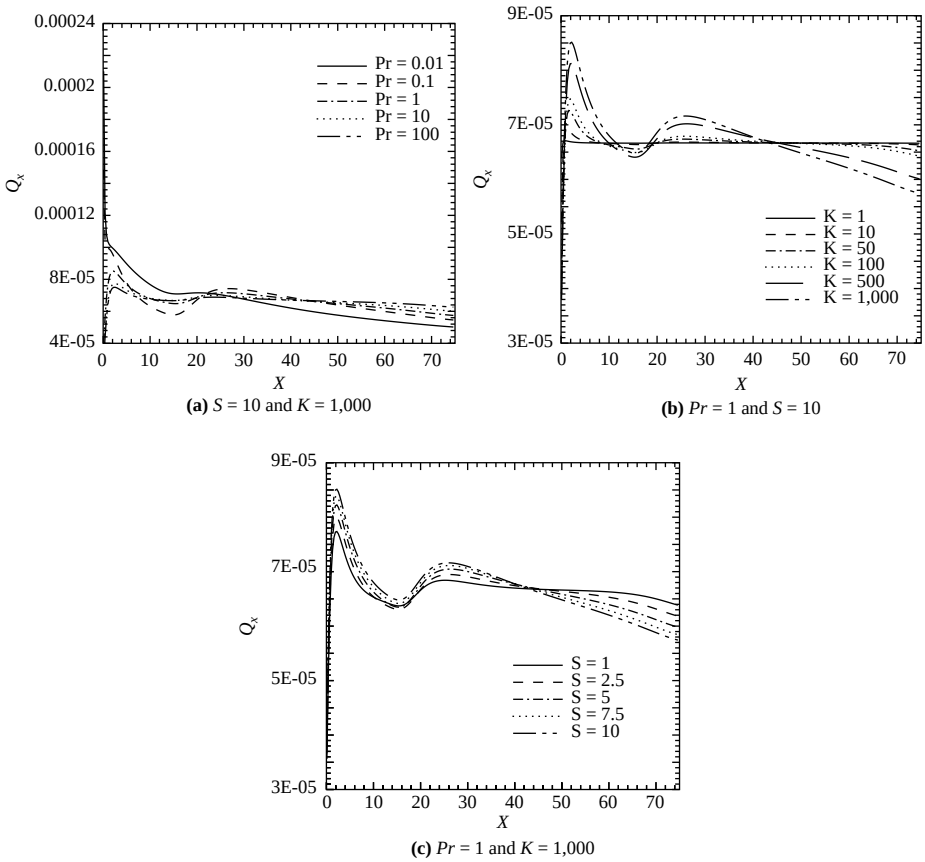

(a) $S = 10$ and $K = 1{,}000$

(b) $Pr = 1$ and $S = 10$

(c) $Pr = 1$ and $K = 1{,}000$

Figure 5.
Heat flux distribution

S (thickness of solid slab)	Thermal conductivity ratio K (k_s/k_f)	$\overline{Nu}$ ($Pr = 0.01$)	$\overline{Nu}$ ($Pr = 0.1$)	$\overline{Nu}$ ($Pr = 1$)	$\overline{Nu}$ ($Pr = 10$)	$\overline{Nu}$ ($Pr = 100$)
0 (non-conjugate)	–	1.36885	8.88723	31.6527	73.019	153.062
1	1	1.36751	8.88378	31.6592	73.0218	153.062
1	100	1.34832	8.79847	31.7535	73.085	153.085
1	1,000	1.30349	8.64074	31.729	73.1181	153.106
5	1	1.36634	8.88148	31.66	73.0223	153.063
5	100	1.322	8.71103	31.7363	73.0925	153.089
5	1,000	1.28271	8.47891	31.6082	73.0989	153.106
10	1	1.36575	8.88066	31.6598	73.0223	153.063
10	100	1.30699	8.67783	31.7199	73.0901	153.089
10	1,000	1.27948	8.42292	31.5114	73.0744	153.101

Table I.
Average Nusselt number (Nu) at various Prandtl numbers

occurring from the bottom surface for all the cases. This computation satisfies the overall energy balance.

6. Concluding remarks

In the present case, the conjugate heat transfer involving a turbulent plane wall jet is considered. The bottom surface is maintained at a constant heat flux boundary condition. The parameters considered are the conductivity ratio, the solid slab thickness and the Prandtl number. The Reynolds number considered is 15,000 because the flow becomes fully turbulent and is independent of the Reynolds number. The non-dimensionalization of the heat flux boundary condition for a conjugate heat transfer case has been done. The non-dimensional bottom surface temperature is high for high Pr fluid and vice versa. As K increases, it decreases whereas it increases with the increase in S. Similar trend is observed for the distribution of the interface temperature. The Nusselt number computed based on the interface temperature increases with Pr because of the thinning of the thermal boundary layer. It is observed that for the range of K and S, Nu_x distribution superimposes with each other. The local heat flux increases near the inlet because Nu_x is large and decreases at the later part to satisfy the equality of heat flux coming from the bottom wall and the heat flux dissipated by the wall jet. The average heat flux at the interface has been computed and found to be equal with average heat flux at the bottom which ensures the overall heat balance.

References

Biswas, G. (2002), "The κ-ϵ model, the RNG κ-ϵ model and the phase-averaged model", in Biswas, G. and Eswaran, V. (Eds), *Turbulent Flows: Fundamentals, Experiments and Modeling*, Chapter 11, Narosa Publishing House, New Delhi, pp. 339-75.

Bouainouche, M., Bourabaa, N. and Desmet, B. (1997), "Numerical study of the wall shear stress produced by the impingement of a plane turbulent jet on a plate", *International Journal of Numerical Methods for Heat and Fluid Flow*, Vol. 7, pp. 548-64.

Glauert, M.B. (1956), "The wall jet", *Journal of Fluid Mechanics*, Vol. 1, pp. 625-43.

Heck, U., Fritsching, U. and Bauckhage, K. (2001), "Fluid flow and heat transfer in a gas jet quenching of a cylinder", *International Journal of Numerical Methods for Heat and Fluid Flow*, Vol. 11, pp. 36-49.

Holland, J.T. and Liburdy, J.A. (1990), "Measurements of the thermal characteristics of heated offset jets", *International Journal of Heat and Mass Transfer*, Vol. 33 No. 1, pp. 69-78.

Hsieh, K.J. and Lien, F.S. (2005), "Conjugate turbulent forced convection in a channel with an array of ribs", *International Journal of Numerical Methods for Heat and Fluid Flow*, Vol. 15, pp. 462-82.

Iaccarino, G., Ooi, A., Durbin, P.A. and Behnia, M. (2002), "Conjugate heat transfer predictions in two-dimensional ribbed passages", *International Journal of Heat and Fluid Flow*, Vol. 23, pp. 340-5.

Kanna, P.R. and Das, M.K. (2005), "Conjugate forced convection heat transfer from a flat plate by laminar plane wall jet flow", *International Journal of Heat and Mass Transfer*, Vol. 48 No. 14, pp. 2896-910.

Kassab, A., Divo, E., Heidmann, J., Steinthorsson, E. and Rodriguez, F. (2003), "Conjugate turbulent forced convection in a channel with an array of ribs", *International Journal of Numerical Methods for Heat and Fluid Flow*, Vol. 13, pp. 581-610.

Launder, B.E. and Spalding, D.B. (1974), "The numerical computation of turbulent flows", *Computer Methods in Applied Mechanics and Engineering*, Vol. 3, pp. 269-89.

Luikov, A.V., Aleksashenko, V.A. and Aleksashenko, A.A. (1971), "Analytical methods of solution of conjugated problems in convective heat transfer", *International Journal of Heat and Mass Transfer*, Vol. 14, pp. 1047-56.

Merci, B., Vierendeels, J., de Langhe, C. and Dick, E. (2003), "Numerical simulation of heat transfer of turbulent impinging jets with two-equation turbulence models", *International Journal of Numerical Methods for Heat and Fluid Flow*, Vol. 13, pp. 110-32.

Patankar, S.V. (1980), *Numerical Heat Transfer and Fluid Flow*, Hemisphere, New York, NY.

Seban, R.A. and Back, L.H. (1961), "Velocity and temperature profiles in a wall jet", *International Journal of Heat and Mass Transfer*, Vol. 3, pp. 255-65.

Versteeg, H.K. and Malalasekera, W. (1996), *An Introduction to Computational Fluid Dynamics. The Finite Volume Method*, Longman, Harlow.

Yilbas, B.S., Shuja, S.Z. and Budair, M.O. (2002), "Jet impingement onto a cavity", *International Journal of Numerical Methods for Heat and Fluid Flow*, Vol. 12 No. 7, pp. 817-38.

Yilbas, B.S., Shuja, S.Z. and Budair, M.O. (2003), "Jet impingement onto a hole with constant wall temperature", *Numerical Heat Transfer: Part A*, Vol. 43 No. 8, pp. 843-65.

Appendix 1. Deriving the expression for heat flux in the fluid side

At the interface between the solid and fluid, the following conditions are applied:

- $\theta_s = \theta_f$ at the interface.
- Heat transfer across the interface must be equal.

Wall heat flux in the fluid side is given by:

$$Q_f = \frac{(\theta_\omega - \theta_{p,f})c((3/4)/\mu)k((1/2)/n)}{\mathrm{Pr}_t\left((1/k)\log(EY^+) + P_f\right)}. \tag{A1}$$

where P_f pee-function, which is given by:

$$P_f = 9.24\left[\left(\frac{Pr}{Pr_t}\right)^{3/4} - 1\right] \times \left[1 + 0.28\exp\left(-0.007\frac{Pr}{Pr_t}\right)\right]. \tag{A2}$$

Heat transfer in the solid side is given by:

$$Q_s = -\frac{1}{RePr}\left(\frac{k_s}{k_f}\right)\frac{\partial\theta}{\partial Y} = \frac{1}{RePr}\left(\frac{k_s}{k_f}\right)\frac{\theta_{p,s} - \theta_\omega}{\Delta Y}. \tag{A3}$$

Interface temperature is calculated by equating equations (A1) and (A3). where $\theta_{p,f}$, $\theta_{p,s}$ are neighbor temperatures in the fluid and solid regions.

Appendix 2. Definition of the constant heat flux at the solid wall

Heat flux at the bottom of the wall is given by:

$$q_b = -k_s\frac{\partial T}{\partial y}. \tag{A4}$$

Since the heat flux across the wall is non-dimensionalized by the $Q_{\mathrm{ref}} = \rho c_p U_0 \Delta T$. Here, ΔT is

some assumed temperature difference. So the same reference heat flux is used to non-dimensionalized equation (A4). Finally, equation (A4) becomes:

$$q_b = -\frac{k_s}{k_f}\frac{\partial\theta}{\partial Y}\frac{1}{Re\cdot Pr}. \tag{A5}$$

In the present calculations Reynolds number is constant in all cases. In order to give the same heat flux at the bottom wall in all cases Q_b is taken as $1/Re$ (heat flux applied $Q_b = 1/Re$).

Appendix 3. Deriving the expression for Nusselt number calculation

$$Nu_x = \frac{h_c H}{k} = h_c(\bar{T}_\omega - \bar{T}_\infty) \times \frac{\nu}{\alpha}.\frac{1}{pC_p}.\frac{1}{U_0(\bar{T}_\omega - \bar{T}_\infty)}.\frac{U_0 H}{\nu}, \tag{A6}$$

$$Nu_x = \frac{Q_\omega Pr\cdot Re}{pC_p(\bar{T}_\omega - \bar{T}_\infty)}. \tag{A7}$$

We can write the above equation as:

$$Nu_x = \frac{Q_\omega Pr\cdot Re}{pC_p(\bar{T}_\omega - \bar{T}_\infty)}.\frac{(\bar{T}_h - \bar{T}_\infty)}{T_h - \bar{T}_\infty} \tag{A8}$$

Finally:

$$Nu_x = \frac{Q_{\omega,n} Pr\cdot Re}{\bar{\theta}_\omega}, \tag{A9}$$

since $\bar{\theta}_\infty = 0$.

Which is used for calculating the Local Nusselt number distribution. The average Nusselt number is calculated as:

$$\overline{Nu} = \frac{1}{L}\int_0^L Nu_x \mathrm{d}x. \tag{A10}$$

Corresponding author
Manab Kumar Das can be contacted at: manab@iitg.ernet.in; manab@mech.iitkgp.ernet.in